
Numerical modeling of the temporal response of back-gated metal-semiconductor-metal photodetector in an equilibrium condition

A. Habibpour^{1*}, N. Das² and H. R. Mashayekhi³

¹*Department of physics, Islamic Azad University, Kazerun Branch, Kazerun, Iran*

²*Department of Electrical and Computer Engineering, Curtin University, Australia*

³*Faculty of Science, University of Kerman, Kerman, Iran*

E-mail: A.habibpoor@gmail.com

Abstract

We have simulated the carrier concentration and temporal response characteristics of a Back-Gated Metal-Semiconductor-Metal (BG-MSM) photodetector in one dimension as a function of optical pulse position on the active region in an equilibrium condition (without bias voltage to the photodetector). We have adopted a nonlinear ambipolar transport model to simulate the behavior of photo-generated carriers in the active region of the BG-MSM photodetector. From the simulation results, it is observed that for optical pulse positions in the cathode region, the magnitude of the response current is exactly the same but opposite that of the anode region. The response of the photodetector is zero when a pulse is positioned at the center of the active region. This important feature of the device could make it attractive for micro-scale positioning of highly sensitive instruments. Our simulation results agreed well with the experimental results.

Keywords: BG-MSM Photodetector; equilibrium condition; ambipolar transport; simulation

1. Introduction

The Back-Gated Metal-Semiconductor-Metal (BG-MSM) photodetector is essentially a three terminal device with high-speed responses. The top two contacts are designed in the same way as usual MSM photodetector and the third contact (the back-gating) is designed to remove the slow holes from the high-speed MSM circuit (Hurd et al., 1996). When the back-gated contact is disconnected from the external circuit (i.e., like a floating condition), the device behaves as a typical MSM structure. In this paper, we are investigating the behavior of this device under varying the optical pulse position, when the third terminal is disconnected from the external circuit, consequently acting as a simple MSM photodetector. A basic MSM photodetector uses a layer of semiconductor material that is sensitive to the wavelength of interest. The metal electrodes are deposited on the top of this layer. Each set of electrodes forms a Schottky barrier contact with the semiconductor, so an MSM photodetector is comprised of back-to-back Schottky diodes. A Schottky diode exhibits a rectified I-V characteristic like *p-n* junctions, but occurs at certain metal-semiconductor junctions (Berger, 1996). A simple schematic diagram of a GaAs BG-MSM photodetector under illumination

is shown in Fig. 1. The two top contacts are made from N^+ GaAs. The electron concentration in the N^+ GaAs layer is comparable with that in metals, so that this type of material is conductive as a metal. The inter-contact layer is intrinsic gallium arsenide (GaAs), which acts as an active medium in the photodetector structure and detects optical pulses. In recent years, owing to the interest of MSM photodetectors for the application in optical sampling, ultrafast and broad-band optical communication systems, as well as their application for the generation of high-power microwave/millimeter waves have been analyzed. (Wilson et al., 1996; Shi et al., 2001).

Experimentally, BG-MSM photodetector demonstrates different temporal responses in the equilibrium condition when the position of optical pulse changes on the surface of I-region (i.e., active region) as shown in Fig. 1. For the same distance from the center of the I-region, the temporal response of the device to a pulse of laser beam impinging around the cathode contact is equal and opposite to that of the anode contact. The temporal response is cancelled when the position of optical pulse is at the center of I-region as shown in the Fig. 2 (Mashayekhi, 1999). This characteristic of the device has an application in the modern nanotechnology such as micro-scale adjusting or positioning of instruments as well as a micro-scale

*Corresponding author

positioning of sensors. By attaching a photodetector to the body of the target object and shining a beam of laser light on the active region, any micro-scale change in the position of the target object will cause a change in the level of photocurrent. If we set the target position to zero when the light hits at the center of the active region, then any displacement of the target from the zero position will correspond to a change in the photocurrent. In Fig. 2, the photocurrent is shown between the maximum and minimum region, the changes are almost linear with the position. This phenomenon suggests that the photocurrent can be scaled to show the displacement of the target on which the photodetector is mounted.

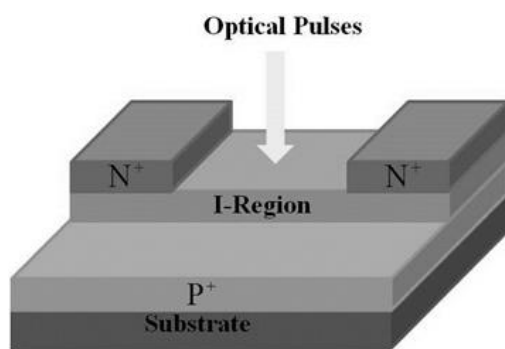


Fig. 1. A simple schematic diagram of a BG-MSM photodetector under illumination

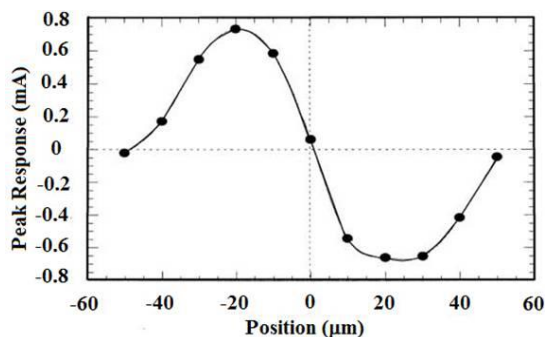


Fig. 2. Experimental results of peak response of a GaAs BG-MSM photodetector as a function of beam position on a 40 μm gap I-region to a laser beam of 580 nm wavelength in the equilibrium condition

We have used a time-dependent nonlinear ambipolar transport equation to simulate the carrier concentration and photocurrent in the equilibrium condition (Neaman, 2003). This equation was applied in the static condition to simulate the behavior of MSM photodetector under varying the optical pulse position (Habibpour, 2011). However, in this paper we found that the applied formulation effectively describes the behavior of device in the equilibrium condition as in the static condition. The position of the optical pulse changes across the active region with 10 μm steps. The device

behavior is analyzed based on a one-dimensional (1-D) simulation of the nonlinear ambipolar transport equation, which includes ambipolar diffusion and bulk recombination. From the simulation results, it has been observed that the device peak response changes sinusoidally by moving the optical pulse position from the anode towards the cathode region.

2. Analysis of carrier transport

Several authors reported that the MSM photodetector could be modeled as a 1D structure (Harder et al., 1990; Sze et al., 1971; Koscielniak et al., 1989; Sarto et al., 1997). In applied voltage condition, this approach can easily be justified if the absorption depth of an incident photon is much less than the inter-contact spacing (I-region length), so that the curvature of the electric field lines between the contacts is small, while the field is approximately constant. In fact, this condition is often satisfied in most experimental situations, since the absorption of photons deep in the substrate is typically avoided as it reduces the detector's responsivity and bandwidth (Sarto et al., 1997). Considering visible lights around the wavelength of 580 nm, the absorption depth δ of the GaAs photodetector is approximately 0.11 μm, which means that the most incident photons are absorbed near the surface. In equilibrium condition, the MSM photodetector has a completely symmetrical structure and it can be considered as a one-dimensional structure. Once photocarriers are created into the I-region, they diffuse into the I-region due to their concentration gradients. Since the electrons have larger mobility, larger diffusion coefficient, they move faster than the holes. Electrons and holes will therefore partly separate and this causes the formation of an internal electric field between the two sets of particles (Streetman, 1980; Wurfel, 2005). This internal electric field couples the photogenerated electron pulse and the photogenerated hole pulse. As a result, the electrons are slowed down and the holes are accelerated. This couple motion is referred to as ambipolar diffusion (Neaman, 2003; Wurfel, 2005).

The ambipolar transport equation in one dimension and without applying any external field (i.e., no bias condition) has reached the following formula (Neaman, 2003)

$$D' \frac{\partial^2 (\delta n(x,t))}{\partial x^2} + g - R = \frac{\partial (\delta n(x,t))}{\partial t} \quad (1)$$

$\delta n(x,t) \approx \delta p(x,t)$

where, D' is the ambipolar diffusion coefficient, g and R are the generation and recombination rates, respectively. The parameter D' can be explained by

the following equation:

$$D' = \frac{D_n D_p (n + p)}{D_n n + D_p p} \quad (2)$$

$$p = p_0 + \delta p \quad (3)$$

$$n = n_0 + \delta n \quad (4)$$

where, p and n are the hole and electron carrier concentrations, p_0 and n_0 are the hole and electron carrier thermal equilibrium concentrations, respectively. The carriers' diffusion constant is determined by the following equation (Einstein relation) (Fichtner et al., 1983):

$$D_{n,p} = \frac{kT}{e} \mu_{n,p} \quad (5)$$

the carrier mobilities μ_n and μ_p are determined via their dependence to the doping level in I-region, so μ_n and μ_p are equal to $8000 \text{ cm}^2 \text{ s}^{-1} \text{ v}^{-1}$ and $400 \text{ cm}^2 \text{ s}^{-1} \text{ v}^{-1}$, respectively (Bhattacharya, 1994).

Carrier recombination is modeled using non-radiative Shockley-Hall-Read (SHR) recombination formula (Fichtner et al., 1983; Bae-Lev, 1984; Masszi et al., 1986):

$$R = \frac{(pn - n_i^2)}{[(p + n_i)\tau_n + (n + n_i)\tau_p]} \quad (6)$$

where, τ_n and τ_p are electron and hole lifetime and assumed to be $1 \times 10^{-10} \text{ s}$ and $3 \times 10^{-10} \text{ s}$, respectively. For the boundary conditions, we assume an infinite surface recombination velocity at the contacts that produce the carrier densities in thermal equilibrium (Iverson, 1987).

3. Simulation setup

In this section, we want to calculate the device response to a beam of laser pulse hitting on different locations between the two top contacts in equilibrium condition. It is assumed that the initial time condition for any optical pulse position is $t_0 = 0$. By making the following definite assumptions, equation (1) has been solved numerically using Matlab software to obtain carrier concentrations as well as photocurrents.

The active layer of the device is a low p-type ($1 \times 10^{20} \text{ m}^{-3}$). In these simulations, a shallow acceptor concentration of $2 \times 10^{20} \text{ m}^{-3}$ and a shallow donor concentration of $0.5 \times 10^{20} \text{ m}^{-3}$ are chosen to give an equilibrium hole density of

$1 \times 10^{20} \text{ m}^{-3}$ in the active region. We have used 100 1D mesh points to represent the length, $L = 40 \text{ }\mu\text{m}$ in the active region.

We assume that the laser pulse has a spot size of $20 \times 10^{-6} \text{ m}$ and a peak height equivalent to a band-to-band generation rate at the illumination surface of $\approx 2.7 \times 10^{29} \text{ (electron-hole) m}^{-3} \text{ s}^{-1}$. Since, the time period of the optical pulse is about 5 ps, this gives a peak of electron and hole density approximately equal to $1 \times 10^{18} \text{ m}^{-3}$ in the active layer. Since the time period of the optical pulse is very short, we can consider the generation only to take place at $t = 0$ and that there is no generation in the latter time steps.

At first, the equation (1) is solved numerically to obtain the photogenerated carrier densities of the BG-MSM photodetector. The obtained carrier densities are then numerically integrated over the length L to yield the temporal response current. The current is calculated using the following formula (Sarto et al., 1997):

$$I(t) = \frac{dQ}{dt} = \frac{e}{L} \int_0^L D \frac{\partial(\delta n(x, t))}{\partial x} dx \quad (7)$$

Figure 3 shows several normalized photocurrent versus the optical pulse position characteristics. The optical pulse position is assumed to be varied from $-30 \text{ }\mu\text{m}$ to $30 \text{ }\mu\text{m}$ in $10 \text{ }\mu\text{m}$ steps. It is noticeable that in equation (7), the term of $\frac{\partial(\delta n(x, t))}{\partial x}$ is in

fact the slope of the photocarriers density curve, and the integral means adding up all possible quantities for this term over the I-region. Obviously, this term can possess a negative quantity as well as a positive quantity, and consequently it can cause an overall negative or positive photocurrent depending on the values which are added up.

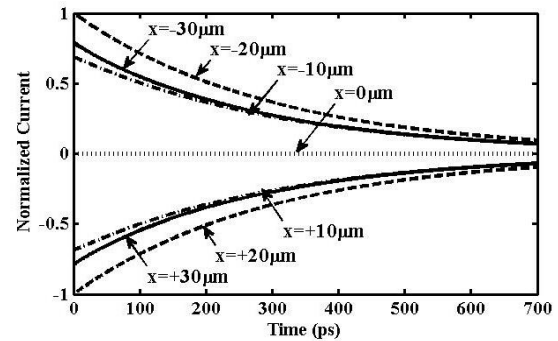


Fig. 3. The normalized photocurrents versus time for optical pulse position at $-30, -20, -10, 0$ (i.e., center), $10, 20$ and $30 \text{ }\mu\text{m}$ relative to the center of the I-region

The simulated peak of normalized photocurrent versus the optical pulse/beam position characteristics is shown in Fig. 4.

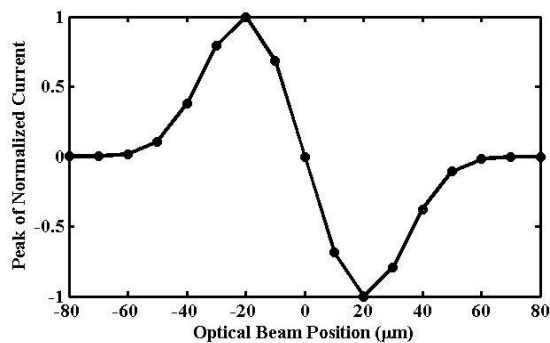


Fig. 4. The peak of normalized photocurrent of the simulated device responses as a function of optical beam position on a 40 μm gap device in the equilibrium condition

It can be observed from Figs. 3 and 4 that the peak response of the device increases as the laser pulse gets closer to either contact. Moreover, the magnitudes of the peaks are asymmetric around the middle of the device. In other words, the flow of photo-current due to the laser pulse of the anode side of the device is the same but opposite to that of the cathode side.

4. Conclusions

We have numerically simulated and analyzed the one-dimensional behavior of a GaAs BG-MSM photodetector as a function of optical pulse position in the equilibrium condition. Nonlinear ambipolar transport model was used to describe the behavior of photogenerated carriers and the photocarrier density, and photocurrent of the BG-MSM photodetector were calculated. From the simulation results, we observed that when the position of the laser spot is near to one of the top two contacts the peak response of the current is increased, because in this situation more carriers are collected in that contact. However, when the laser spot center is overlapped with the center of I-region (active region), the total diffusion current is canceled. These results are in good agreement with the experimental ones.

Acknowledgment

The authors would like to thank Adrian Boland-Thoms for his kindness in reviewing this article.

References

Hurd, C. M., & Mckinnon, W. R. (1996). Modeling a

- backgated GaAs Metal-Semiconductor-Metal photodetector. *Journal of Applied Physics*, 80(9), 5449.
- Berger, P. R. (1996). Metal-Semiconductor-Metal Photodetectors. *IEEE Potentials*, 28.
- Wilson, S. P., & Walker, A. B. (1996). Scaling properties of metal - semiconductor - metal photodetectors. *Journal of Semiconductor Science Technology*, 11, 1322–1327
- Shi, J. W., Gan, K. G., Chiu, Y. J., & et al. (2001). Metal-semiconductor-metal traveling-wave photodetectors. *IEEE Photonics Technology Letters*, 16(6), 623–625.
- Mashayekhi, H. R. (1999). Theoretical and Experimental studies of Back - Gated Metal - semiconductor - metal photodetectors. PhD dissertation, Essex University (Essex, UK).
- Neaman, D. A. (2003). *Semiconductor Physics and Devices: basic principles, 3rd edition*. McGraw-Hill Inc.
- Habibpoor, A., & Mashayekhi, H. R. (2011). Numerical modeling of the effect of optical pulse position on the impulse response of a Metal-Semiconductor-Metal (MSM) photodetector (low field condition). *European Physical Journal of Applied Physics*, 55, 10502.
- Harder, Ch. S., Zeghbroeck, B. J. V., Kesler, M. P., & Meier, H. P., et al. (1990). High speed GaAs/AlGaAs optoelectronic devices for computer applications. *IBM Journal of Research and Development*, 34(4), 568–584.
- Sze, S. M., Coleman, D. J., & Loya, A. (1971). Current transport in metal-semiconductor-metal (MSM) structures. *Journal of Solid State Electronics*, 14, 1209–1218.
- Koscielniak, W. C., Pelouard, J. L., & Littlejohn, M. A. (1989). Dynamic behavior of photocarriers in a GaAs metal-semiconductor-metal photodetector with sub-half-micron electrode pattern. *Applied Physics Letter*, 54, 567–569.
- Sarto, A. W., & Zeghbroeck, B. J. V. (1997). Photocurrents in a Metal-semiconductor-metal photodetector. *IEEE Journal of Quantum Electronics*, 33(12), 2188–2189.
- Streetman, B. G. (1980). *Solid State Electronic Devices, 2nd edition*. Englewood Cliffs, N. J., Prentice Hall.
- Wurfel, P. (2005). *Physics of Solar Cells*. WILY-VCH verlay GmbH & Co. KGaA, Weinheim.
- Fichtner, W., Rose, D. J., & Bank, R. E. (1983). Semiconductor Device Simulation. *IEEE Transactions on Electronic Devices*, ED 30(9), 1020, 1022.
- Bhattacharya, P. (1994). *Semiconductor Optoelectronic Devices*. Prentice Hall Inc.
- Bae-Lev, A. (1984). *Semiconductors and Electronic Devices, 2nd edition*. Prentice-Hall International (U.K) Ltd.
- Masszi, F., Tove, P. A., Bohline, J., & Nord, H. (1986). Computer modeling and comparison of different rectifier(m-s, m-s-m, p-n⁺) diodes. *IEEE Transaction on Electronic Devices*, ED 33(4), 469.
- Iverson, A. E., & Smith, D. L. (1987). Mathematical modeling of photodetector transient response. *IEEE Transactions on Electronic Devices*, ED 34(10), 2098.